10-2-2015

The Nicotine Metabolite, Cotinine, Alters the Assembly and Trafficking of a Subset of Nicotinic Acetylcholine Receptors

Ashley M. Fox
University of Kentucky, ashley.loe@uky.edu

Faruk H. Moonschi
University of Kentucky, faruk.moonschi@uky.edu

Christopher I. Richards
University of Kentucky, chris.richards@uky.edu

The Nicotine Metabolite, Cotinine, Alters the Assembly and Trafficking of a Subset of Nicotinic Acetylcholine Receptors

Notes/Citation Information
Published in *The Journal of Biological Chemistry*, v. 290, no. 40, p. 24403-24412.

Digital Object Identifier (DOI)
https://doi.org/10.1074/jbc.M115.661827

THE JOURNAL OF BIOLOGICAL CHEMISTRY VOL. 290, NO. 40, pp. 24403–24412, October 2, 2015

The Nicotine Metabolite, Cotinine, Alters the Assembly and Trafficking of a Subset of Nicotinic Acetylcholine Receptors*

Received for publication, April 27, 2015, and in revised form, August 10, 2015 Published, JBC Papers in Press, August 12, 2015, DOI 10.1074/jbc.M115.661827

Ashley M. Fox, Faruk H. Moonschi, and Christopher I. Richards[1]

From the Department of Chemistry, University of Kentucky, Lexington, Kentucky 40506

Background: Nicotine-induced changes in nAChRs are linked to nicotine addiction.
Results: Cotinine, the primary metabolite of nicotine, alters the assembly and expression of some subtypes of nAChRs.
Conclusion: Cotinine affects trafficking and assembly of a subset of nAChRs.
Significance: Cotinine has a much longer half-life in the body than nicotine, and therefore may contribute to physiological effects attributed to nicotine.

Exposure to nicotine alters the trafficking and assembly of nicotinic receptors (nAChRs), leading to their up-regulation on the plasma membrane. Although the mechanism is not fully understood, nicotine-induced up-regulation is believed to contribute to nicotine addiction. The effect of cotinine, the primary metabolite of nicotine, on nAChR trafficking and assembly has not been extensively investigated. We utilize a pH-sensitive variant of GFP, super ecliptic pHluorin, to differentiate between intracellular nAChRs and those expressed on the plasma membrane to quantify changes resulting from cotinine and nicotine exposure. Similar to nicotine, exposure to cotinine increases the number of $\alpha4\beta2$ receptors on the plasma membrane and causes a redistribution of intracellular receptors. In contrast to this, cotinine exposure down-regulates $\alpha6\beta2\beta3$ receptors. We also used single molecule fluorescence studies to show that cotinine and nicotine both alter the assembly of $\alpha4\beta2$ receptors to favor the high sensitivity $(\alpha4)_2(\beta2)_3$ stoichiometry.

Nicotinic acetylcholine receptors (nAChRs)[2] are cation-selective ligand-gated ion channels that express throughout the central and peripheral nervous systems. They form pentameric structures composed of α ($\alpha2$-$\alpha10$) and β ($\beta2$-$\beta4$) subunits, with each subunit encoded by a distinct gene (1–3). Receptor assembly into the correct stoichiometry and composition is essential for proper subcellular localization, agonist sensitivity, and Ca^{2+} permeability (4, 5). Nicotine, the primary addictive component in tobacco, binds to and activates nAChRs. Beyond eliciting a functional response, nicotine has been shown to up-regulate some nAChR subtypes including those composed of $\alpha4$ and $\beta2$ subunits. Up-regulation has been defined as changes in stoichiometry, distribution, or increased number of nAChRs (6–9) and has been established as one of the consequences of chronic nicotine exposure (7, 8, 10–12). Nicotine-induced changes in nAChRs have been proposed as a potential component in the mechanism for nicotine addiction (8, 13–17). The current pharmacological chaperoning hypothesis suggests that these changes only require concentrations of nicotine to be high enough to interact with the specific subtype in the endoplasmic reticulum, meaning surface activation is not required (8, 18) Other nAChR ligands, including drugs that have been evaluated as smoking cessation agents, have also been shown to up-regulate nAChRs. These drugs include the partial agonists cytisine (19) and varenicline (20) as well as the antagonist mecamylamine (21). Although nicotine exposure increases the assembly of the high sensitivity receptor, $(\alpha4)_2(\beta2)_3$ (16, 22), cytisine has been shown to alter the stoichiometry of $\alpha4\beta2$ with a preference for the low sensitivity receptor, $(\alpha4)_3(\beta2)_2$, potentially due to the existence of an additional binding site for cytisine at the α-α interface (23, 24). The high and low sensitivity stoichiometries of $\alpha4\beta2$ exhibit different ligand binding affinities and Ca^{2+} flux and desensitize at different rates (5, 9). These differences, along with the increased expression of the high sensitivity stoichiometry, are believed to contribute to nicotine addiction (8, 25, 26).

In humans, ~80% of nicotine is metabolized to cotinine, which has a much longer pharmacological half-life (24 h) than nicotine (2 h) (27, 28). Nicotine and cotinine are very similar in structure, varying by only an acetyl group (29). Cotinine is also known to cross the blood-brain barrier (30), where it acts as a partial agonist to nAChRs (31). Studies have shown that cotinine improves learning, memory, and attention as well as enhances cognition and executive function (29, 32). Additionally, cotinine exposure on its own has not been shown to lead to addictive behavior or to the negative cardiovascular effects associated with nicotine (33). As a result, cotinine has generated interest as a pharmacologically active compound, with a few recent studies that examine the effect of cotinine on nAChRs (32, 34, 35). Terry *et al.* (34) recently found that 1 μM cotinine in combination with low levels of acetylcholine sensitized $\alpha7$ nAChRs, resulting in increased channel activity as compared with acetylcholine alone. They also found that 10 μM cotinine exposure for 48 h led to a slight down-regulation of $\alpha4\beta2$ in a *Xenopus laevis* oocyte expression system (34). Here

* This work was supported in part by the National Institute on Drug Abuse (NIDA) Training Grant DA016176 (to A. M. F.) and NIDA Grant DA038817 (C. I. R.). The authors declare that they have no conflicts of interest with the contents of this article.
[1] To whom correspondence should be addressed: Dept. of Chemistry, University of Kentucky, 505 Rose St., Lexington, KY 40506. Tel.: 859-218-0971; E-mail: chris.richards@uky.edu.
[2] The abbreviations used are: nAChR, nicotinic acetylcholine receptor; ER, endoplasmic reticulum; N2a, neuroblastoma 2a; PM, plasma membrane; % PM, percentage on plasma membrane; PMID, plasma membrane integrated density; SEP, super-ecliptic pHluorin; TIRF, total internal reflection fluorescence; TIRFM, total internal reflection fluorescence microscopy.

we utilize a combination of super ecliptic pHluorin-based fluorescence imaging and single molecule measurements to show that although high concentrations of cotinine (>5 μM) do not increase receptor expression on the plasma membrane, lower concentrations of cotinine alter both the assembly and the trafficking of nAChRs.

Experimental Procedures

Reagents—(−)Cotinine and (−)-nicotine hydrogen tartrate salt were obtained from Sigma-Aldrich.

Nicotinic Receptor Plasmid Constructs—All constructs were preassembled as described previously (36). All subunit plasmids are of mouse origin. Super ecliptic pHluorin (SEP) fluorophores were incorporated on the C terminus of α4 and α6 subunits. GFP fluorophores were incorporated into the M3-M4 loop of the α4 subunit. All plasmids assemble normally and have been used in previous studies (14, 36). Plasmids containing nAChRs labeled on the C terminus with SEP have previously been shown to be functional based on whole cell patch clamp studies (7, 22, 36). The QuikChange II XL site-directed mutagenesis kit was used to create the α5-D398N mutation commonly associated with an increase in risk of smoking and lung cancer. The D398N corresponds to an aspartic acid to asparagine change in position 397 in the mouse plasmid (37).

Cell Culture and Transfection—Undifferentiated mouse neuroblastoma 2a (N2a) cells were cultured using standard tissue culture techniques and maintained in growth media consisting of DMEM and Opti-MEM, supplemented with 10% fetal bovine serum, penicillin, and streptomycin (19, 36). Cells were plated by adding 90,000 cells to poly-D-lysine-coated 35-mm glass bottom dishes (In Vitro Scientific). The following day, growth medium was replaced with Opti-MEM for cell transfection. Cells were transfected with 500 ng of each nAChR subunit plasmid mixed in 250 μl of Opti-MEM. A separate aliquot of 2 μl of Lipofectamine-2000 and 250 μl of Opti-MEM was incubated at room temperature for 5 min and then combined with the plasmid solution for an additional 25 min before being added to pre-plated N2a cells. After 24 h at 37 °C, the transfection mixture was replaced with growth media and incubated for an additional 24 h at 37 °C before imaging. For drug-exposed cells, the indicated concentration of the appropriate drug was added at the time of the transfection and replenished in the growth medium replacement for a total of 48 h of exposure before imaging. Transfection efficiency was ~80% and was not influenced by the presence of a drug.

Total Internal Reflection Fluorescence Microscopy (TIRFM)—Samples were imaged with objective style total internal reflection fluorescence microscopy with an inverted fluorescence microscope (Olympus ix83). TIRFM allows the excitation of fluorophores within ~100–200 nm from the cell-glass bottom dish interface, visualizing receptors localized to the plasma membrane or peripheral endoplasmic reticulum (38). SEP was excited with a 488-nm diode-pumped solid-state laser (~1.00 watt/cm^2) through the objective (Olympus, 1.49NA, 60× oil immersion) and detected by an electron-multiplying charge coupled device (Andor iXon Ultra 897). To obtain total internal reflection, the laser was focused on the back aperture of the objective lens and the angle was adjusted using a stepper motor to translate the beam laterally across the objective lens. Due to low excitation intensity, photobleaching is not an issue on the timescale of these measurements.

Measuring Receptor Expression and Trafficking—The pH sensitivity of SEP was utilized to determine subcellular location within the TIRF field. SEP undergoes 488 nm excitation at neutral pH but is dark under acidic conditions of pH < 6 (39), allowing us to differentiate between intracellular and inserted nAChRs. The SEP tag is fused with the C terminus of the nAChR subunit so that it is exposed to the pH on the luminal side of the organelles within the secretory pathway. Before imaging, growth medium was exchanged for extracellular solution (150 mM NaCl, 4 mM KCl, 2 mM $MgCl_2$, 2 mM $CaCl_2$, 10 mM HEPES, and 10 mM glucose) adjusted to pH 7.4. Receptors in the ER (pH > 7) and on the PM (pH of extracellular solution, 7.4) are visible, whereas those in the lower pH environments of the Golgi and secretory vesicles are not fluorescent (36, 40). After images were collected at pH 7.4, the solution was exchanged with an otherwise identical solution adjusted to pH 5.4. When the pH of the extracellular solution is <6, nAChRs located on the PM transition into the off state, so the observed fluorescence is solely from nAChRs in the peripheral ER (7, 38, 41). The integrated density of TIRF images, showing the relative number of fluorescent receptors, are collected at both pH 7.4 and pH 5.4. The integrated density at pH 5.4 is subtracted from the total integrated density of fluorophores in the ER and on the PM shown at pH 7.4 to determine the integrated density of receptors on the plasma membrane (PMID). The ratio of receptors on the plasma membrane (% PM) is the PMID divided by the total integrated density at pH 7.4 to provide a ratio of receptors within the TIRF view that reside on the membrane. Increased PMID reflects an up-regulation in the number of receptors found on the PM. An increase in the percentage of receptors found on the plasma membrane (% PM) corresponds to a change in the distribution of receptors between the ER and PM.

Real time images were acquired at a frame rate of 200 ms for 1500 frames to capture fusion of nAChR-containing transport vesicles with the plasma membrane. These studies enable us to identify changes in the number of vesicles that contain nAChRs but not in the total number of vesicles. Insertion events were manually counted per cell during a randomly chosen 50 frames (10 s). Insertion events were defined as a burst of fluorescence at the PM lasting at least 2 frames (400 ms) and including lateral spreading of fluorophores to ensure transient full fusion of the vesicle and delivery of nAChRs to the membrane. Persistent, continuously repeating bursts of fluorescence were not counted because a discrete exocytic event could not be guaranteed.

Receptor Expression Data Analysis—Quantification of fluorescence intensity was determined using ImageJ (National Institutes of Health) by manually selecting an intensity-based threshold and region of interest. All figures show results from a single imaging session that are representative of data collected on at least three separate occasions. All graphs show the mean with error bars representing S.E. p values were determined using a two-tailed t test with equal variance not assumed.

Stoichiometric Determination—Vesicles were prepared from HEK-293T cells expressing α4-gfp/β2-wt as described previ-

ously (42) using nitrogen cavitation. Biased transfections were performed by adding unequal amounts of α4-gfp and β2-wt plasmid during the transfection of HEK-293T cells. These control studies were completed using 10:1, 4:1, and 1:4 ratios of α4-gfp to β2-wt plasmid. Equal amounts of plasmid were used for all other studies. Vesicles were immobilized on clean glass bottom dishes functionalized with 1 mg/ml Biotin-PEG-Silane (Laysan Bio, Inc.), 0.05 mg/ml NeutrAvidin (Thermo Scientific), and 1 μg/ml biotinylated anti-GFP antibody. Single vesicles were spatially isolated and immobilized using the GFP in the receptor binding to a substrate-immobilized anti-GFP antibody. Vesicles were imaged using TIRF microscopy while covered in 1 ml of PBS. TIRF microscopy limits excitation to within ~100 nm of the substrate surface, decreasing background fluorescence. Generating small enough vesicles limits the probability of capturing more than one receptor in a single vesicle. This single molecule isolation, as well as immobilization of these vesicles within the TIRF illumination, allows us to perform single receptor measurements. Control experiments using monomeric receptors showed that there was a low probability of having more than one receptor per isolated vesicle. Of the vesicles generated via nitrogen cavitation, ~15% contain a receptor (42). Each field of view was imaged for 500 frames at a frame rate of 200 ms while undergoing continuous 488 nm excitation with an intensity of 60 watt/cm^2. Autofocus (Olympus ZDC2) was used to minimize focal drift. Time traces of 4 × 4-pixel regions of interest were generated using ImageJ with the Time Trace Analyzer V3.0 plugin. Photobleaching steps were determined manually as described previously (42–44). Previously, a discrete bleaching step was confirmed to correspond to one subunit (42, 43). Table 1 includes the number of accepted and rejected spots as well as the complete raw observed distribution of stoichiometry for each condition. Time traces showing continuous decrease in fluorescence intensity or indistinct number of bleaching steps were rejected. GFP fails to mature a small percentage of the time, leading to some subunits not exhibiting typical fluorescence, which would result in the undercounting of bleaching events (42, 44). To account for this, the probability of observing one, two, or three photobleaching steps in the time traces for each stoichiometry was calculated using a custom MATLAB script by fitting data to a binomial distribution, using the probability of GFP fluorescing equal to 0.90 (44). The agreement of theoretical and experimental data was determined using a χ-squared goodness of fit analysis. The probability of observing a specific number of photobleaching steps, for a receptor with fixed number of subunits is calculated using

$$F\,(k, n, p) = \frac{n!}{k!(n-k)!}p^k(1-p)^{n-k} \qquad \text{(Eq. 1)}$$

where n is the total number of labeled subunits, k is the number of observed units, p is the probability of GFP being in an observable state, and F is the probability of observing k number of photobleaching steps from n number of labeled subunits. Modeling the probability of observing a specific number of photobleaching steps for $\alpha4\beta2$ requires two binomial distributions (Eq. 2) for $k = 1$, 2, and 3 for both F_1 and F_2. F_1 corresponds to the case when n_1 GFP-labeled subunits are in a receptor, and F_2 corresponds to the case when there are n_2 GFP-labeled subunits in a receptor.

$$F_{tot} = a_1 \times F_1\,(k, n_1, p) + a_2 \times F_2\,(k, n_1, p) \qquad \text{(Eq. 2)}$$

Results

Up-regulation of $\alpha4\beta2$ Receptors—We used SEP, a pH-sensitive variant of GFP (36, 39, 45), to quantify the up-regulation of $\alpha4\beta2$ nAChRs in the presence of nicotine and cotinine. SEP undergoes 488 nm excitation and exhibits green fluorescence at neutral pH but is not fluorescent under acidic conditions of pH < 6 (39). We exposed N2a cells expressing α4-sep and β2-wt subunits to cotinine concentrations ranging from 50 nm to 10 μM. Fig. 1 shows representative TIRF images of N2a cells expressing α4-sep β2-wt treated with no drug (Fig. 1*A*), 500 nM nicotine (Fig. 1*B*), or 1 μM cotinine (Fig. 1*C*). For all rows, the *first column* shows a cell imaged in TIRF with an extracellular pH of 7.4 (ER and PM fluorescing), the *second column* shows an image of the same cell at pH 5.4 (fluorescence from ER only), and the *third column* shows a subtracted image representing just the PM component. Although the subtracted TIRF footprint shown in the third column qualitatively shows PM expression for the given cells, the extent of up-regulation was quantified by calculating the PMID of $\alpha4\beta2$ receptors with and without cotinine. Distribution of $\alpha4\beta2$ receptors within the cell are compared using percentage of plasma membrane (% PM), calculated by dividing the PM integrated density, determined from the difference between pH 7.4 and pH 5.4 images, by the total integrated density of receptors fluorescing on the PM and ER at pH 7.4. Increased expression on the plasma membrane was observed when cells were treated with as little as 100 nM cotinine, showing a 50% increase in number of receptors on the membrane (Fig. 2*A*; $p < 0.05$), as well as a 25% shift in the distribution (% PM) of receptors toward the membrane (Fig. 2*B*; $p < 0.01$). The highest levels of up-regulation were reached in the presence of 1 μM cotinine, resulting in more than a 2-fold increase in PMID (Fig. 2*A*; $p < 0.001$) and over a 50% shift in distribution toward the PM (Fig. 2*B*; $p < 0.001$). Exposure to 5 μM cotinine showed an increase over no drug, but the effect was much less than observed with 1 μM. Exposure to 10 μM cotinine did not result in an increase in the number of receptors on the PM (Fig. 2*A*), although the distribution of receptors at 10 μM slightly favors the PM (Fig. 2*B*; $p < 0.05$).

Cotinine Increases Number of $\alpha4\beta2$ Insertion Events—We utilized SEP-tagged nAChRs to quantify nAChR-containing vesicle trafficking by measuring the number of vesicle insertion events at the plasma membrane. The SEP tag is oriented on the luminal side of secretory vesicles so that they are maintained at a low pH prior to delivery to the PM. As a result, receptors are not fluorescent as they are trafficked to the PM but turn on as the vesicle fuses with the PM, when the SEP tag is exposed to the extracellular solution (pH 7.4) (39, 45). We defined an insertion event as a burst of fluorescence appearing at the plasma membrane, which corresponds to membrane insertion of an SEP-tagged nAChR. After the initial insertion event, a lateral spread of fluorescence was observed corresponding to full fusion of the vesicle and subsequent diffusion of the labeled receptors. We counted insertion events in cells expressing $\alpha4\beta2$, $\alpha4\beta2\alpha5$, or

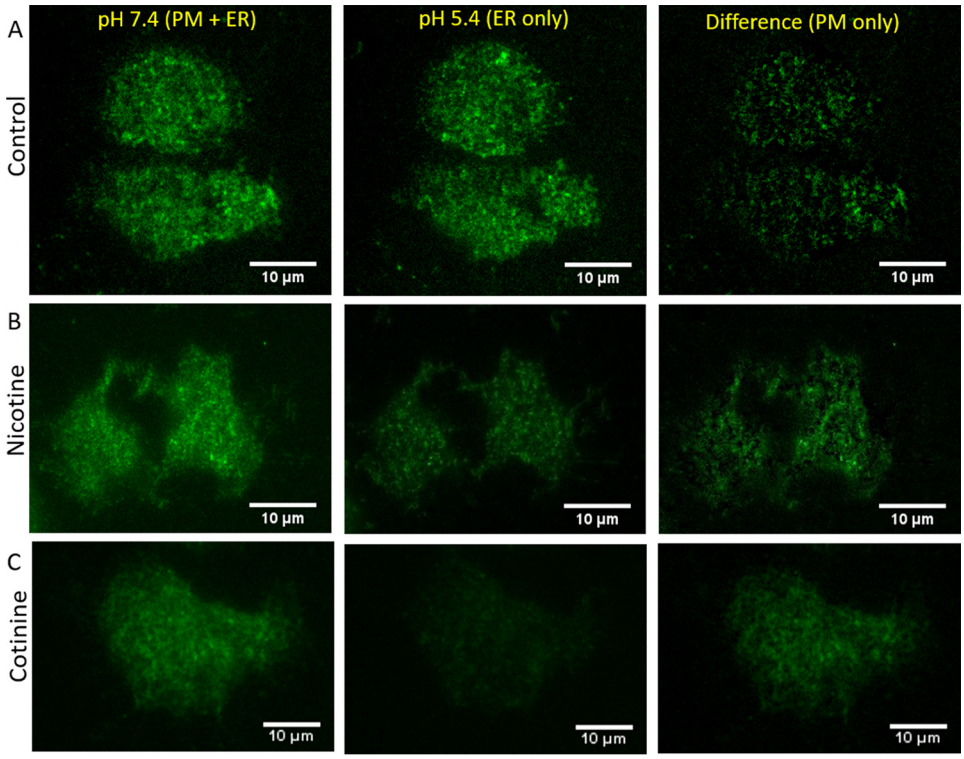

FIGURE 1. **TIRFM images illustrating increased $\alpha4\beta2$ PMID with nicotine or cotinine exposure.** *A–C*, representative TIRFM images of α4-sep β2-wt with no drug (*A*), 500 nM nicotine (*B*), or 1 μM cotinine (*C*). The *first column* shows respective cells at pH 7.4 with receptors on the plasma membrane and endoplasmic reticulum fluorescing, whereas the *second column* shows the same cells at pH 5.4 with all fluorescence from receptors in the endoplasmic reticulum. The *third column* shows images constructed by subtracting the pH 5.4 image from the pH 7.4 image, resulting in receptors located on the plasma membrane (PMID).

$\alpha4\beta2\alpha5$-D398N as compared with those exposed to no drug or 1 μM cotinine. Fig. 3*B* shows a representative series of images of an insertion event, illustrating frames prior to insertion (Fig. 3*B*, *panel 1*), during arrival of the vesicle shown as a burst of fluorescence (Fig. 3*B*, *panel 2*), followed by a lateral spread (Fig. 3*B*, *panels 3–6*) and diffusion across the membrane (Fig. 3*B*, *panels 7–9*). Cells treated with 1 μM cotinine exhibited approximately a 30% increase in the number of vesicles that contained $\alpha4\beta2$ as compared with untreated cells (Fig. 3*C*). When the α5D or α5N auxiliary subunit was coexpressed with $\alpha4$ and $\beta2$ subunits, there were no differences in the trafficking rate of nAChRs in the presence of cotinine.

Cotinine Exposure Results in Preferential Assembly of $(\alpha4)_2(\beta2)_3$—Because nAChRs are pentameric, $\alpha4\beta2$ can assemble with either an $(\alpha4)_3(\beta2)_2$ or an $(\alpha4)_2(\beta2)_3$ stoichiometry. We used a technique that our laboratory recently developed to perform single molecule analysis of subunit stoichiometry by spatially isolating nAChRs embedded in cell membrane-derived vesicles (42). We generated vesicles from cells expressing α4-gfp and β2-wt subunits. These vesicles were isolated on glass substrates, and TIRF microscopy was used to visualize the GFP fluorescence signal (Fig. 4*A*). We used single step photobleaching of GFP to identify the number of α4-gfp subunits in each receptor. The number of bleaching steps corresponds to the number of GFP-tagged subunits present and, therefore, indicates the stoichiometry of the receptor (22, 44). Examples of two bleaching steps (Fig. 4*B*) corresponding to two α4-gfp subunits and $(\alpha4)_2(\beta2)_3$ stoichiometry, or three bleaching steps (Fig. 4*C*) indicating $(\alpha4)_3(\beta2)_2$ stoichiometry, are shown.

We plotted the distribution of individual vesicles showing one, two, or three bleaching steps. The total distribution of observed bleaching steps including the total number of vesicles accepted or rejected is included in Table 1. For cells not exposed to any compound, binomial distributions weighted for 60% $(\alpha4)_3(\beta2)_2$ and 40% $(\alpha4)_2(\beta2)_3$ fit the observed distribution (Fig. 4*D*). Treatment with 500 nM nicotine altered the stoichiometric distribution with a shift toward a higher percentage of receptors with the high sensitivity stoichiometry. The distribution of nicotine-exposed cells was best fit for binomial distributions weighted with 35% $(\alpha4)_3(\beta2)_2$ and 65% $(\alpha4)_2(\beta2)_3$ (Fig. 4*E*). We repeated these experiments in the presence of 1 μM cotinine. This also resulted in a shift in the stoichiometric distribution toward $(\alpha4)_2(\beta2)_3$. The observed distribution fit to binomials weighted 30% $(\alpha4)_3(\beta2)_2$ and 70% $(\alpha4)_2(\beta2)_3$ (Fig. 4*F*). Fig. 5 compares the stoichiometries derived from the weighted fits (Fig. 4, *d–f*) of $\alpha4\beta2$ with no drug, nicotine, and cotinine. Exposure to either nicotine or cotinine results in the preferential assembly of the high sensitivity $(\alpha4)_2(\beta2)_3$ receptor.

Previous studies have altered the primary stoichiometry of $\alpha4\beta2$ expressed using biased transfection, with one subunit expressed at higher levels than the other (4, 5, 19, 46). These types of studies have primarily used *Xenopus* oocyte expression systems with changes in stoichiometry determined from changes in the biphasic dose response based on whole cell current measurements. To verify our observations of nicotine- and cotinine-induced changes in $(\alpha4)_3(\beta2)_2$ stoichiometry, we performed stoichiometry measurements with biased transfection

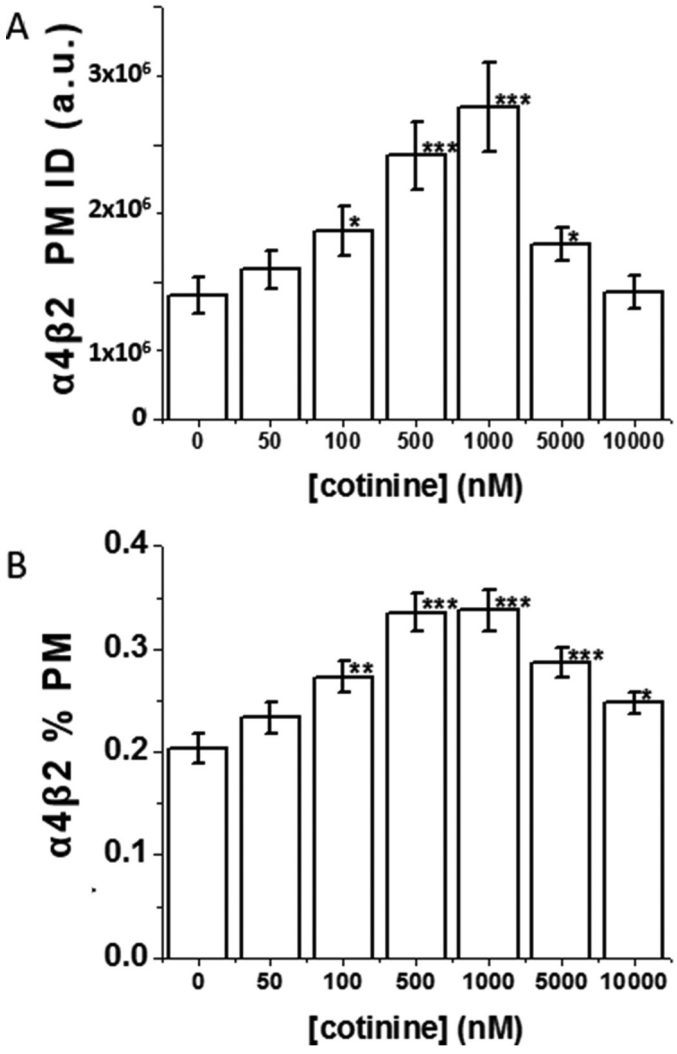

FIGURE 2. **Cotinine-induced up-regulation of α4β2.** *A*, quantification of α4β2 PMID (*A*) shows an up-regulation of α4β2 receptors with exposure to as little as 100 nM cotinine. *a. u.*, arbitrary units. *B*, cotinine also alters the distribution of receptors within the field of view, as shown by an increase in % PM for α4β2 in N2a cells treated with cotinine (n = 40, 21, 21, 23, 13) Data are mean values ± S.E. (**, $p < 0.01$, ***, $p < 0.001$).

ratios of 10:1, 4:1, 1:1, and 1:4 (α4:β2). Single molecule analysis showed that the fraction of $(\alpha4)_3(\beta2)_2$ reduced and the fraction of $(\alpha4)_2(\beta2)_3$ increased when higher levels of β2 were transfected (1:4 (α4:β2)) (Fig. 6).

Low Concentrations of Cotinine Decrease α6β2β3 Receptor Density on the PM—We also evaluated the effect of cotinine on the expression of α6β2 and α6β2β3 nAChRs. Matching previous studies (7), our data also show that incorporation of the β3 subunit into an α6β2 pentamer results in increased expression levels on the PM (Fig. 7; $p < 0.05$). Once β3 is included in the pentamer, there appears to be a cotinine concentration-dependent response resulting in lower levels of α6β2β3 nAChR on the plasma membrane. At low levels of cotinine (100 nM), there is a trend toward a decreased number of α6β2β3 nAChRs, reaching significance with 500 nM cotinine (Fig. 7; $p < 0.05$). The down-regulated level of expression of α6β2β3 with 500 nM cotinine is comparable with that of α6β2 when the β3 subunit is absent. Down-regulation was less pronounced when cotinine treatment was increased to 1 μM cotinine and was lost at 5 μM cotinine as PMID is comparable with α6β2β3 with no drug.

Cotinine Does Not Alter Density or Trafficking of α6β2, α4β2α5, or α3β4 receptors—Although α6β2β3 exhibited down-regulation as a result of cotinine exposure, we found that cotinine had no effect on the membrane expression of α6β2. SEP-based studies show no significant differences in PM integrated density or the percentage expressed on the plasma membrane for α6β2 exposed to cotinine (Fig. 8*A*). Likewise, PMID and % PM of α4β2α5, α4β2α5-D398N (Fig. 8, *B–D*), α3β4, α3β4α5, and α3β4α5-D398N (Fig. 9) did not change upon the addition of 500 nM nicotine or 1 μM cotinine, although we did observe a cotinine-independent difference in the distribution of α4β2α5-398N as compared with 398D with an increase in the fraction of observable receptors on the plasma membrane as compared with the peripheral ER.

Discussion

It is well established that chronic nicotine exposure up-regulates and alters the assembly of α4β2 nAChRs (10–12, 47), but the effects of nicotine metabolites on nAChR assembly and trafficking are not well studied. We exposed cells to physiologically relevant levels of cotinine matching the average reported values of cotinine in a smoker's blood, urine, or brain (48–50). Our data show that cotinine up-regulates α4β2 nAChRs at concentrations of 1 μM cotinine, which corresponds to the average concentration of cotinine in the blood of a typical smoker (48). Cotinine induces significant increases in both α4β2 PMID and % PM at as little as 100 nM. This suggests that cotinine could potentially contribute to α4β2 up-regulation in smokers because brain concentrations of cotinine are estimated to be ~300 nM (28). However, at higher concentrations of cotinine, this up-regulation effect is lost, suggesting a secondary effect that depresses PM expression. Cotinine acts as a partial agonist of nAChRs, activating channels at higher concentrations. It has also been shown that nAChR ligands at higher concentrations can result in endocytosis (51). The highest concentrations (10 μM) used in our studies may be sufficient to cause endocytosis of α4β2 nAChRs, resulting in a decrease of observed receptors on the PM.

Due to the observed increase in the number of α4β2 receptors located on the plasma membrane, we speculated that the increase in receptors at lower concentrations of cotinine could be partially due to an increase in the trafficking of receptors to the PM. We found that 1 μM cotinine increases the number of single vesicle insertion events, which suggests that cotinine, similar to nicotine, increases the trafficking of α4β2 from the ER to the PM. Therefore, the higher PMID and % PM levels resulting from cotinine exposure are at least partially the result of increased frequency of insertion of vesicles containing α4β2 receptors.

It has also been shown that nicotine exposure results in a preferential assembly of high sensitivity α4β2 receptors with an $(\alpha4)_2(\beta2)_3$ stoichiometry (22). In the absence of nicotine or cotinine, the fifth position of the pentamer slightly favors occupation by an α subunit. In the presence of cotinine or nicotine, α4β2 preferentially assembles the high sensitivity $(\alpha4)_2(\beta2)_3$ stoichiometry. This alteration does not require surface recep-

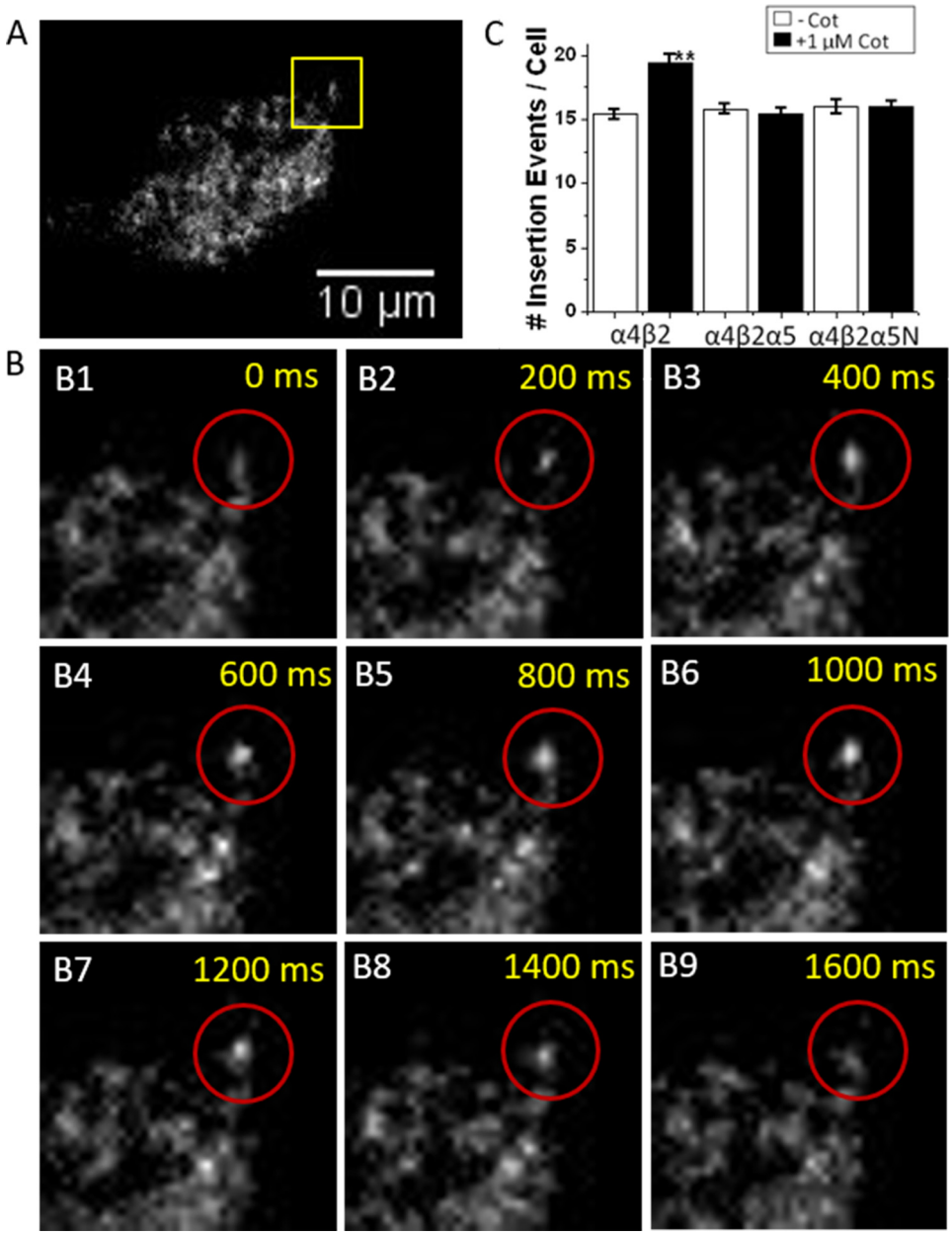

FIGURE 3. **Increased number of $\alpha4\beta2$ single vesicle insertion events when exposed to 1 μM cotinine.** *A*, TIRFM image of an N2a transfected with α4-sep β2-wt exposed to 1 μM cotinine (*cot*). Images were collected at a 200-ms frame rate and analyzed over 10 s. An example of an insertion event is shown in *B*, where *panel 1* is the frame before the insertion and *panel 2* shows vesicle arrival, followed by a lateral spread (*panels 3–6*) and diffusion across the membrane (*panels 7–9*). *C*, insertion events were counted for α4-sep β2-wt, α4-sep β2-wt α5-wt, or α4-sep β2-wt α5-D398N with or without exposure to 1 μM cotinine for 48 h, showing an increase in frequency in insertion for $\alpha4\beta2$ exposed to cotinine. ($n = 5$) Data are mean values $\pm$ S.E. (**, $p < 0.01$).

tor-activating concentrations of nicotine, but is thought to be linked to the mechanism of nicotine addiction.

Changes in nAChR number, stoichiometry, and trafficking are well established consequences of exposure to nicotine (8, 10, 12, 36, 47). It is possible that cotinine-induced up-regulation results from a similar mechanism as nicotine, likely acting inside the cell by binding immature subunits to enhance the maturation and stabilization of nAChRs (18, 52). This chaperoning process is not unique to nicotine, and can potentially occur with any ligand that readily permeates cell membranes and interacts with intracellular nAChRs. This is consistent with our observations of nAChRs exposed to cotinine, which is a partial agonist of $\alpha4\beta2$ (31, 53).

In the case of nicotine, up-regulation is subtype-specific. It appears that subtypes with a higher basal PM density are not subjected to nicotine-induced up-regulation, possibly because receptor transport is already efficient. For instance, basal levels of $\alpha3\beta4$ nAChRs are three times higher than $\beta2$-containing nAChRs and have not been shown to up-regulate when exposed to concentrations of nicotine seen in smokers (14, 36), but can up-regulate at much higher concentrations (13). If cotinine affects nAChRs in a similar mechanism, $\alpha3\beta4$ may not be up-regulated by cotinine because of the already high levels of PM expression.

Although $\alpha4\beta2$ shows clear up-regulation when exposed to nicotine, contradicting results have been reported for $\alpha6\beta2$*,

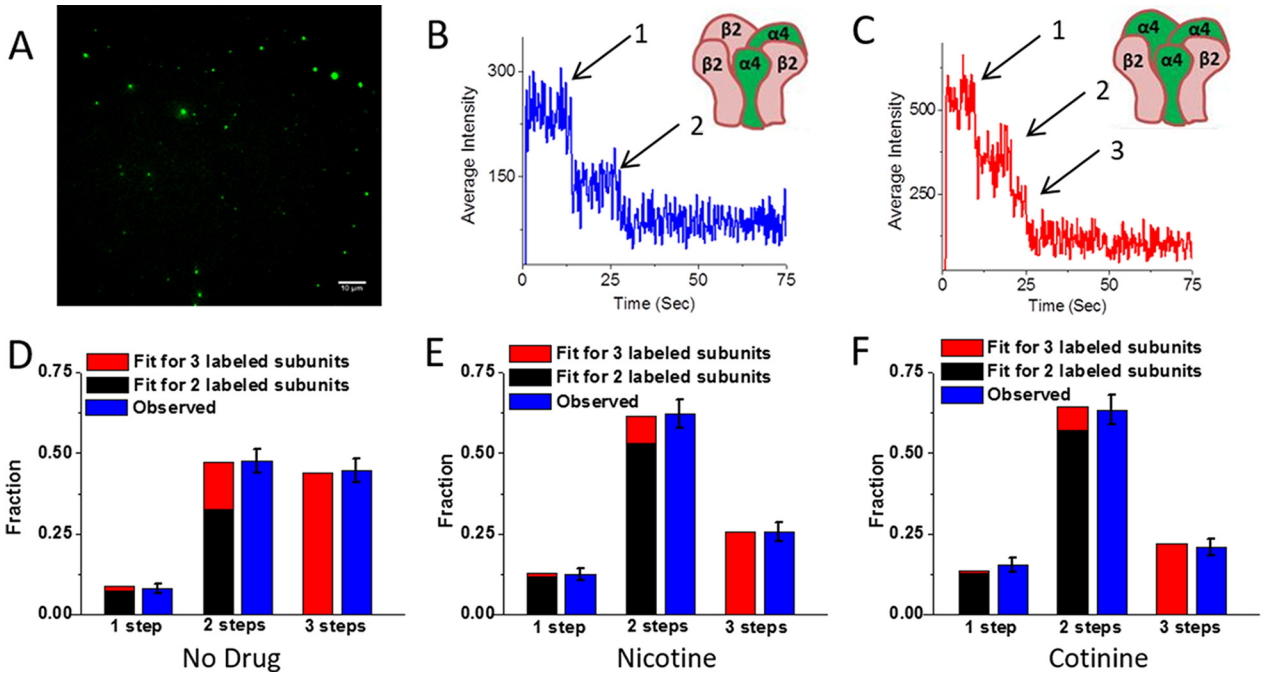

FIGURE 4. **Cotinine exposure results in preferential assembly of $(\alpha4)_2(\beta2)_3$.** *A*, cell-derived vesicles containing a single nAChR were isolated and immobilized on a glass coverslip and then imaged using TIRFM. Because one fluorophore corresponds to the presence of one GFP-tagged subunit in an assembled receptor, the number of bleaching steps corresponds to the number of α-GFP subunits. *B*, time traces for two bleaching steps correspond to the presence of 2 α4-gfp subunits, and thus to $(\alpha4)_2(\beta2)_3$ stoichiometry. *C*, three bleaching steps correspond to $(\alpha4)_3(\beta2)_2$ stoichiometry. Observed and fitted distributions of number of bleaching steps for α4-gfp/β2-wt are shown. *D*, no drug exposure results in nearly equal amounts of $(\alpha4)_2(\beta2)_3$ and $(\alpha4)_3(\beta2)_2$ stoichiometry. *E* and *F*, exposure to nicotine alters this distribution to 65% $(\alpha4)_2(\beta2)_3$ and 35% $(\alpha4)_3(\beta2)_2$ stoichiometry (*E*), whereas cotinine exposure results in a 70% $(\alpha4)_2(\beta2)_3$ and 30% $(\alpha4)_3(\beta2)_2$ distribution (*F*). The *error bars* for subunit distribution are based on counting events and are calculated as the square root of the counts.

TABLE 1

Total distribution of observed bleaching steps including the total number of spots accepted and rejected as well as the number of one-, two-, three-, and four-step bleaching events observed for all three conditions

	No. of vesicles	One step	Two steps	Three steps	Four steps	Rejected
No drug	903	28	171	160	12	532
+ Cotinine (1 μM)	782	47	194	64	10	467
+ Nicotine (500 nM)	800	40	202	83	11	464

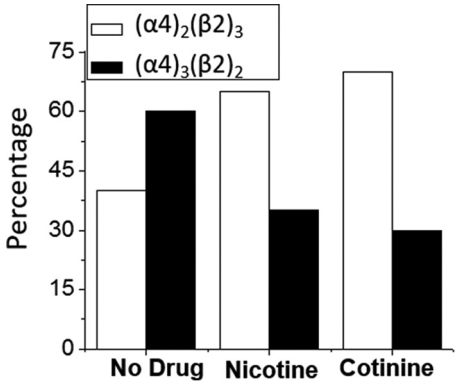

FIGURE 5. **Drug-induced changes in assembly of $\alpha4\beta2$.** Nicotine and cotinine exposure causes a higher percentage of α4β2 nAChRs to be assembled with $(\alpha4)_2(\beta2)_3$ stoichiometry. When no drug is present, 40% of α4β2 has $(\alpha4)_2(\beta2)_3$ stoichiometry, whereas 60% has $(\alpha4)_3(\beta2)_2$. This distribution is changed to 65% $(\alpha4)_2(\beta2)_3$ and 35% $(\alpha4)_3(\beta2)_2$ in the presence of nicotine and 70% $(\alpha4)_2(\beta2)_3$ and 30% $(\alpha4)_3(\beta2)_2$ in the presence of cotinine.

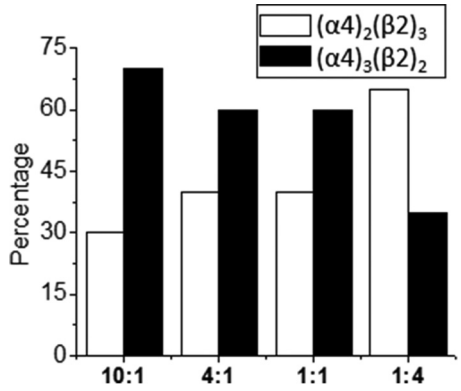

FIGURE 6. **Biased transfection as a control for changes in stoichiometry.** The ratios listed on the *x* axis represent the transfected ratio of (α4:β2). Biased transfection at a 1:4 ratio (α4:β2) resulted in a clear shift toward the $(\alpha4)_2(\beta2)_3$ stoichiometry (65%) as compared with unbiased transfection, which results in 40% $(\alpha4)_2(\beta2)_3$ based on the distribution of single receptor bleaching steps. Biased transfection of 4:1 toward α4 did not result in changes in the distribution of stoichiometries as compared with unbiased transfection. However, biased transfection of 10:1 toward α4 did shift the stoichiometry toward the $(\alpha4)_3(\beta2)_2$ stoichiometry from 60% when unbiased to 70% when biased.

with claims of up-regulation, down-regulation, or no change when chronically exposed to nicotine (54–56). These discrepancies may be due to the presence or absence of the auxiliary β3 subunit and a dose-dependent response of α6β2β3 to nicotine (7). Our data also show that the incorporation of a β3 auxiliary subunit resulted in higher levels of expression on the PM as compared with α6β2 alone, as well as a dose-dependent down-regulation of α6β2β3 in the presence of cotinine. Recent evi-

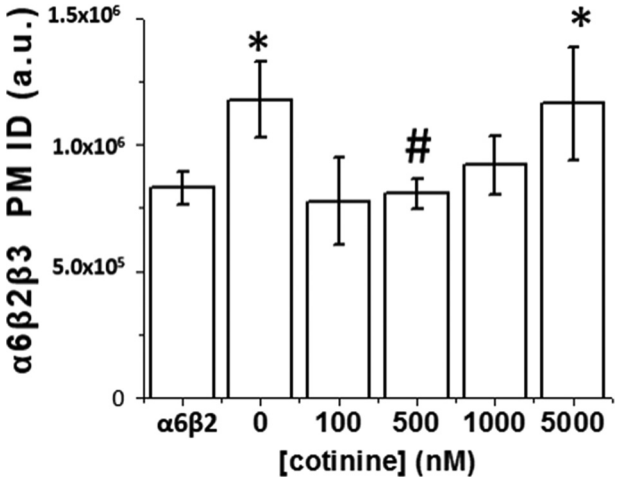

FIGURE 7. **Cotinine-induced down-regulation of $\alpha6\beta2\beta3$.** Quantification of PMID for $\alpha6\beta2\beta3$ as compared with a control with no $\beta3$ subunit, $\alpha6\beta2$, shows a significant increase in the number of receptors on the membrane when $\beta3$ is incorporated into the $\alpha6\beta2$ pentamer. When $\beta3$ is present, 500 nM cotinine significantly decreases the PMID, with a trend toward down-regulation at 100 nM cotinine. Down-regulation is less pronounced when cotinine treatment was increased to 1 μM cotinine and is lost at 5 μM cotinine as PMID is comparable with $\alpha6\beta2\beta3$ with no drug (n = 19, 27, 16, 11, 11). Data are mean values ± S.E. (*, $p < 0.05$ as compared with control of $\alpha6\beta2$; #, $p < 0.05$ as compared with control of $\alpha6\beta2\beta3$ with no drug). *a. u.*, arbitrary units.

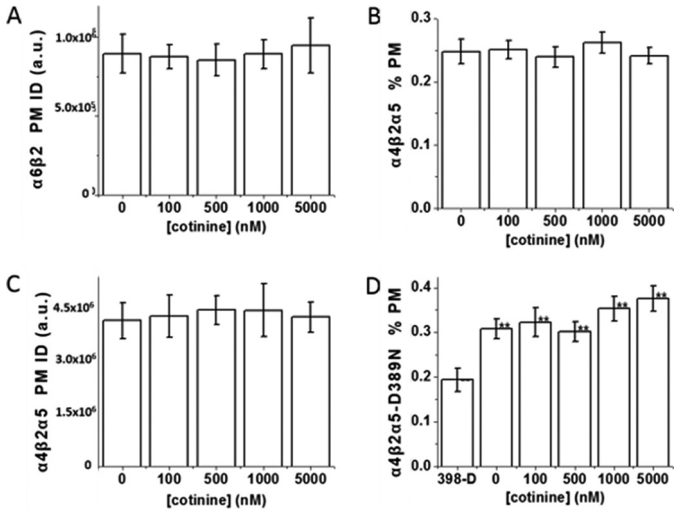

FIGURE 8. **Cotinine does not affect $\alpha6\beta2$- or $\alpha5$-containing nAChRs.** *A*, cotinine does not alter the expression of $\alpha6\beta2$ (n = 18, 11, 9, 18, 8). *a. u.*, arbitrary units. *B* and *C*, incorporation of $\alpha5$ results in loss of up-regulation after treatment with cotinine in terms of number of receptors (*C*) and distribution toward the membrane (*B*) (n = 19, 21, 20, 10, 37). *D*, the distribution of receptors containing an $\alpha5$-D398N subunit is altered to a higher % PM, regardless of the concentration of cotinine, whereas the number of receptors remains unchanged (n = 14, 23, 26, 33, 24, 30). Data are mean values ± S.E. (**, $p < 0.01$).

dence suggests that a KKK motif within the $\beta3$ subunit plays a regulatory role in $\alpha6\beta2$* expression (7). This motif is essential for nicotine-induced up-regulation of $\alpha6\beta2\beta3$, possibly acting as a recognition site for COPI binding (7). Cotinine potentially differs in its interaction with the KKK motif as compared with nicotine. Interestingly, another study has shown that cotinine only interacts with a subset of $\alpha6\beta2$*, whereas the entire population is sensitive to nicotine (53). The lack of cotinine-induced up-regulation of $\alpha6\beta2\beta3$ is potentially related to its action on only a portion of this receptor population. This effect could also

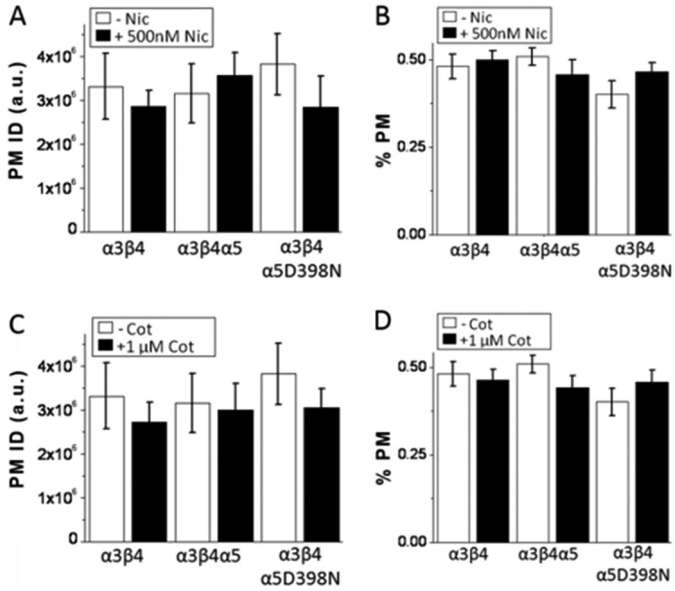

FIGURE 9. **Nicotine and cotinine do not affect trafficking of $\alpha3\beta4$.** *A* and *B*, no changes in number (*A*) or distribution (*B*) of $\alpha3\beta4$, $\alpha3\beta4\alpha5$, or $\alpha3\beta4\alpha5$D398N were seen when exposed to 500 nM nicotine (*Nic*, n = 13, 14, 11, 11, 4, 8). *a. u.*, arbitrary units. *C* and *D*, exposure to 1 μM cotinine (*Cot*) also resulted in no changes in $\alpha3\beta4$, $\alpha3\beta4\alpha5$, or $\alpha3\beta4\alpha5$D398N PMID (*C*) or % PM (*D*) (n = 13, 14, 11, 7, 4, 18). Data are mean values ± S.E.

partially explain discrepancies between groups that detect up-regulation (7, 55, 56) or down-regulation (57) in varying brain regions based on concentrations of nicotine or cotinine present.

These studies show that nicotine's primary metabolite, cotinine, has a similar effect on the trafficking and assembly of nAChRs as seen with nicotine. Cotinine has a longer half-life and higher sustained concentration than nicotine in the human body. It is possible that variations in the concentration of cotinine resulting from gene variation and clearance rates in different ethnicities could account for some differences in rates of nicotine addiction.

Author Contributions—A. M. F. and C. I. R. designed the studies and wrote the paper. A. M. F and F. H. M. performed the experiments. F. H. M. wrote the analysis software for the single molecule studies. All authors reviewed the results and approved the final version of the manuscript.

References

1. Albuquerque, E. X., Pereira, E. F. R., Alkondon, M., and Rogers, S. W. (2009) Mammalian nicotinic acetylcholine receptors: from structure to function. *Physiol. Rev.* **89,** 73–120
2. Anand, R., Conroy, W. G., Schoepfer, R., Whiting, P., and Lindstrom, J. (1991) Neuronal nicotinic acetylcholine-receptors expressed in *Xenopus* oocytes have a pentameric quaternary structure. *J. Biol. Chem.* **266,** 11192–11198
3. Lukas, R. J., Changeux, J. P., Le Novère, N., Albuquerque, E. X., Balfour, D. J., Berg, D. K., Bertrand, D., Chiappinelli, V. A., Clarke, P. B., Collins, A. C., Dani, J. A., Grady, S. R., Kellar, K. J., Lindstrom, J. M., Marks, M. J., Quik, M., Taylor, P. W., and Wonnacott, S. (1999) International Union of Pharmacology. XX. Current status of the nomenclature for nicotinic acetylcholine receptors and their subunits. *Pharmacol. Rev.* **51,** 397–401
4. Zwart, R., and Vijverberg, H. P. (1998) Four pharmacologically distinct subtypes of $\alpha4\beta2$ nicotinic acetylcholine receptor expressed in Xenopus

laevis oocytes. *Mol. Pharmacol.* **54,** 1124–1131
5. Moroni, M., Zwart, R., Sher, E., Cassels, B. K., and Bermudez, I. (2006) $\alpha4\beta2$ nicotinic receptors with high and low acetylcholine sensitivity: pharmacology, stoichiometry, and sensitivity to long-term exposure to nicotine. *Mol. Pharmacol.* **70,** 755–768
6. Miwa, J. M., Freedman, R., and Lester, H. A. (2011) Neural systems governed by nicotinic acetylcholine receptors: emerging hypotheses. *Neuron* **70,** 20–33
7. Henderson, B. J., Srinivasan, R., Nichols, W. A., Dilworth, C. N., Gutierrez, D. F., Mackey, E. D. W., McKinney, S., Drenan, R. M., Richards, C. I., and Lester, H. A. (2014) Nicotine exploits a COPI-mediated process for chaperone-mediated up-regulation of its receptors. *J. Gen. Physiol.* **143,** 51–66
8. Lester, H. A., Xiao, C., Srinivasan, R., Son, C. D., Miwa, J., Pantoja, R., Banghart, M. R., Dougherty, D. A., Goate, A. M., and Wang, J. C. (2009) Nicotine is a selective pharmacological chaperone of acetylcholine receptor number and stoichiometry. Implications for drug discovery. *AAPS J.* **11,** 167–177
9. Tapia, L., Kuryatov, A., and Lindstrom, J. (2007) Ca^{2+} permeability of the $(\alpha4)_3(\beta2)_2$ stoichiometry greatly exceeds that of $(\alpha4)_2(\beta2)_3$ human acetylcholine receptors. *Mol. Pharmacol.* **71,** 769–776
10. Colombo, S. F., Mazzo, F., Pistillo, F., and Gotti, C. (2013) Biogenesis, trafficking and up-regulation of nicotinic ACh receptors. *Biochem. Pharmacol.* **86,** 1063–1073
11. Marks, M. J., Burch, J. B., and Collins, A. C. (1983) Effects of chronic nicotine infusion on tolerance development and nicotinic receptors. *J. Pharmacol. Exp. Ther.* **226,** 817–825
12. Marks, M. J., Grady, S. R., Salminen, O., Paley, M. A., Wageman, C. R., McIntosh, J. M., and Whiteaker, P. (2014) $\alpha6\beta2^*$-subtype nicotinic acetylcholine receptors are more sensitive than $\alpha4\beta2^*$-subtype receptors to regulation by chronic nicotine administration. *J. Neurochem.* **130,** 185–198
13. Mazzo, F., Pistillo, F., Grazioso, G., Clementi, F., Borgese, N., Gotti, C., and Colombo, S. F. (2013) Nicotine-modulated subunit stoichiometry affects stability and trafficking of $\alpha3\beta4$ nicotinic receptor. *J. Neurosci.* **33,** 12316–12328
14. Srinivasan, R., Pantoja, R., Moss, F. J., Mackey, E. D. W., Son, C., Miwa, J., and Lester, H. A. (2011) Nicotine upregulates $\alpha4\beta2$ nicotinic receptors and ER exit sites via stoichiometry-dependent chaperoning. *J. Gen. Physiol.* **137,** 59–79
15. Lomazzo, E., Hussmann, G. P., Wolfe, B. B., Yasuda, R. P., Perry, D. C., and Kellar, K. J. (2011) Effects of chronic nicotine on heteromeric neuronal nicotinic receptors in rat primary cultured neurons. *J. Neurochem.* **119,** 153–164
16. Nelson, M. E., Kuryatov, A., Choi, C. H., Zhou, Y., and Lindstrom, J. (2003) Alternate stoichiometries of $\alpha4\beta2$ nicotinic acetylcholine receptors. *Mol. Pharmacol.* **63,** 332–341
17. Changeux, J. P. (2010) Nicotine addiction and nicotinic receptors: lessons from genetically modified mice. *Nat. Rev. Neurosci.* **11,** 389–401
18. Srinivasan, R., Henderson, B. J., Lester, H. A., and Richards, C. I. (2014) Pharmacological chaperoning of nAChRs: A therapeutic target for Parkinson's disease. *Pharmacol. Res.* **83,** 20–29
19. Srinivasan, R., Richards, C. I., Dilworth, C., Moss, F. J., Dougherty, D. A., and Lester, H. A. (2012) Forster resonance energy transfer (FRET) correlates of altered subunit stoichiometry in Cys-loop receptors, exemplified by nicotinic $\alpha4\beta2$. *Int. J. Mol. Sci.* **13,** 10022–10040
20. Turner, J. R., Castellano, L. M., and Blendy, J. A. (2011) Parallel anxiolytic-like effects and upregulation of neuronal nicotinic acetylcholine receptors following chronic nicotine and varenicline. *Nicotine Tob. Res.* **13,** 41–46
21. Pauly, J. R., Marks, M. J., Robinson, S. F., van de Kamp, J. L., and Collins, A. C. (1996) Chronic nicotine and mecamylamine treatment increase brain nicotinic receptor binding without changing $\alpha4$ or $\beta2$ mRNA levels. *J. Pharmacol. Exp. Ther.* **278,** 361–369
22. Richards, C. I., Luong, K., Srinivasan, R., Turner, S. W., Dougherty, D. A., Korlach, J., and Lester, H. A. (2012) Live-cell imaging of single receptor composition using zero-mode waveguide nanostructures. *Nano Lett.* **12,** 3690–3694
23. Marotta, C. B., Rreza, I., Lester, H. A., and Dougherty, D. A. (2014) Selective ligand behaviors provide new insights into agonist activation of nicotinic acetylcholine receptors. *ACS Chem. Biol.* **9,** 1153–1159
24. Mazzaferro, S., Benallegue, N., Carbone, A., Gasparri, F., Vijayan, R., Biggin, P. C., Moroni, M., and Bermudez, I. (2011) Additional acetylcholine (ACh) binding site at $\alpha4/\alpha4$ interface of $(\alpha4\beta2)2\alpha4$ nicotinic receptor influences agonist sensitivity. *J. Biol. Chem.* **286,** 31043–31054
25. Nashmi, R., Xiao, C., Deshpande, P., McKinney, S., Grady, S. R., Whiteaker, P., Huang, Q., McClure-Begley, T., Lindstrom, J. M., Labarca, C., Collins, A. C., Marks, M. J., and Lester, H. A. (2007) Chronic nicotine cell specifically upregulates functional $\alpha4^*$ nicotinic receptors: basis for both tolerance in midbrain and enhanced long-term potentiation in perforant path. *J. Neurosci.* **27,** 8202–8218
26. Govind, A. P., Vezina, P., and Green, W. N. (2009) Nicotine-induced upregulation of nicotinic receptors: underlying mechanisms and relevance to nicotine addiction. *Biochem. Pharmacol.* **78,** 756–765
27. Moran, V. E. (2012) Cotinine: beyond that expected, more than a biomarker of tobacco consumption. *Front. Pharmacol.* **3,** 173
28. Buccafusco, J. J., and Terry, A. V. (2003) The potential role of cotinine in the cognitive and neuroprotective actions of nicotine. *Life Sci.* **72,** 2931–2942
29. Echeverria, V., and Zeitlin, R. (2012) Cotinine: a potential new therapeutic agent against Alzheimer's disease. *CNS Neurosci. Ther.* **18,** 517–523
30. Riah, O., Courrière, P., Dousset, J.-C., Todeschi, N., and Labat, C. (1998) Nicotine is more efficient than cotinine at passing the blood-brain barrier in rats. *Cell. Mol. Neurobiol.* **18,** 311–318
31. Vainio, P. J., and Tuominen, R. K. (2001) Cotinine binding to nicotinic acetylcholine receptors in bovine chromaffin cell and rat brain membranes. *Nicotine Tob. Res.* **3,** 177–182
32. Terry, A. V., Jr., Hernandez, C. M., Hohnadel, E. J., Bouchard, K. P., and Buccafusco, J. J. (2005) Cotinine, a neuroactive metabolite of nicotine: potential for treating disorders of impaired cognition. *CNS Drug Rev.* **11,** 229–252
33. Benowitz, N. L., Hukkanen, J., and Jacob, P., 3rd. (2009) Nicotine chemistry, metabolism, kinetics and biomarkers. *Handb. Exp. Pharmacol.* **2009,** 29–60, 10.1007/978-3-540-69248-5_2
34. Terry, A. V., Jr., Callahan, P. M., and Bertrand, D. (2015) *R*-(+) and *S*-(−) isomers of cotinine augment cholinergic responses *in vitro* and *in vivo*. *J. Pharmacol. Exp. Ther.* **352,** 405–418
35. Grizzell, J. A., and Echeverria, V. (2014) New insights into the mechanisms of action of cotinine and its distinctive effects from nicotine. *Neurochem. Res.* 10.1007/s11064–014-1359–2
36. Richards, C. I., Srinivasan, R., Xiao, C., Mackey, E. D. W., Miwa, J. M., and Lester, H. A. (2011) Trafficking of $\alpha4^*$ nicotinic receptors revealed by superecliptic phluorin. *J. Biol. Chem.* **286,** 31241–31249
37. Frahm, S., Slimak, M. A., Ferrarese, L., Santos-Torres, J., Antolin-Fontes, B., Auer, S., Filkin, S., Pons, S., Fontaine, J. F., Tsetlin, V., Maskos, U., and Ibañez-Tallon, I. (2011) Aversion to nicotine is regulated by the balanced activity of $\beta4$ and $\alpha5$ nicotinic receptor subunits in the medial habenula. *Neuron* **70,** 522–535
38. Mattheyses, A. L., Simon, S. M., and Rappoport, J. Z. (2010) Imaging with total internal reflection fluorescence microscopy for the cell biologist. *J. Cell Sci.* **123,** 3621–3628
39. Yudowski, G. A., Puthenveedu, M. A., Leonoudakis, D., Panicker, S., Thorn, K. S., Beattie, E. C., and von Zastrow, M. (2007) Real-time imaging of discrete exocytic events mediating surface delivery of AMPA receptors. *J. Neurosci.* **27,** 11112–11121
40. Paroutis, P., Touret, N., and Grinstein, S. (2004) The pH of the secretory pathway: measurement, determinants, and regulation. *Physiology (Bethesda)* **19,** 207–215, 10.1152/physiol.00005.2004
41. Khiroug, S. S., Pryazhnikov, E., Coleman, S. K., Jeromin, A., Keinanen, K., and Khiroug, L. (2009) Dynamic visualization of membrane-inserted fraction of pHluorin-tagged channels using repetitive acidification technique. *BMC Neurosci.* **10,** 141
42. Moonschi, F. H., Effinger, A. K., Zhang, X., Martin, W. E., Fox, A. M., Heidary, D. K., DeRouchey, J. E., and Richards, C. I. (2015) Cell-derived vesicles for single-molecule imaging of membrane proteins. *Angew. Chem. Int. Ed. Engl.* **54,** 481–484
43. Das, S. K., Liu, Y., Yeom, S., Kim, D. Y., and Richards, C. I. (2014) Single-particle fluorescence intensity fluctuations of carbon nanodots.

Nano Lett. **14,** 620–625
44. Ulbrich, M. H., and Isacoff, E. Y. (2007) Subunit counting in membrane-bound proteins. *Nat. Methods* **4,** 319–321
45. Araki, Y., Lin, D. T., and Huganir, R. L. (2010) Plasma membrane insertion of the AMPA receptor GluA2 subunit is regulated by NSF binding and Q/R editing of the ion pore. *Proc. Natl. Acad. Sci. U.S.A.* **107,** 11080–11085
46. Govind, A. P., Walsh, H., and Green, W. N. (2012) Nicotine-induced up-regulation of native neuronal nicotinic receptors is caused by multiple mechanisms. *J. Neurosci.* **32,** 2227–2238
47. Kuryatov, A., Luo, J., Cooper, J., and Lindstrom, J. (2005) Nicotine acts as a pharmacological chaperone to up-regulate human $\alpha4\beta2$ acetylcholine receptors. *Mol. Pharmacol.* **68,** 1839–1851
48. Vine, M. F., Hulka, B. S., Margolin, B. H., Truong, Y. K., Hu, P.-C., Schramm, M. M., Griffith, J. D., McCann, M., and Everson, R. B. (1993) Cotinine concentrations in semen, urine, and blood of smokers and nonsmokers. *Am. J. Public Health* **83,** 1335–1338
49. Ghosheh, O., Dwoskin, L. P., Li, W.-K., and Crooks, P. A. (1999) Residence times and half-lives of nicotine metabolites in rat brain after acute peripheral administration. *Drug Metab. Dispos.* **27,** 1448–1455
50. Caraballo, R. S., Giovino, G. A., Pechacek, T. F., Mowery, P. D., Richter, P. A., Strauss, W. J., Sharp, D. J., Eriksen, M. P., Pirkle, J. L., and Maurer, K. R. (1998) Racial and ethnic differences in serum cotinine levels of cigarette smokers. *JAMA* **280,** 135–139
51. St John, P. A., and Gordon, H. (2001) Agonists cause endocytosis of nicotinic acetylcholine receptors on cultured myotubes. *J. Neurobiol.* **49,** 212–223
52. Henderson, B. J., and Lester, H. A. (2015) Inside-out neuropharmacology of nicotinic drugs. *Neuropharmacology* **96,** 178–193
53. O'Leary, K., Parameswaran, N., McIntosh, J. M., and Quik, M. (2008) Cotinine selectively activates a subpopulation of $\alpha3/\alpha6\beta2$ nicotinic receptors in monkey striatum. *J. Pharmacol. Exp. Ther.* **325,** 646–654
54. Tumkosit, P., Kuryatov, A., Luo, J., and Lindstrom, J. (2006) $\beta3$ subunits promote expression and nicotine-induced up-regulation of human nicotinic $\alpha6^*$ nicotinic acetylcholine receptors expressed in transfected cell lines. *Mol. Pharmacol.* **70,** 1358–1368
55. Perez, X. A., Bordia, T., McIntosh, J. M., Grady, S. R., and Quik, M. (2008) Long-term nicotine treatment differentially regulates striatal $\alpha6\alpha4\beta2^*$ and $\alpha6(non\alpha4)\beta2^*$ nAChR expression and function. *Mol. Pharmacol.* **74,** 844–853
56. Walsh, H., Govind, A. P., Mastro, R., Hoda, J. C., Bertrand, D., Vallejo, Y., and Green, W. N. (2008) Upregulation of nicotinic receptors by nicotine varies with receptor subtype. *J. Biol. Chem.* **283,** 6022–6032
57. Perry, D. C., Mao, D., Gold, A. B., McIntosh, J. M., Pezzullo, J. C., and Kellar, K. J. (2007) Chronic nicotine differentially regulates $\alpha6$- and $\beta3$-containing nicotinic cholinergic receptors in rat brain. *J. Pharmacol. Exp. Ther.* **322,** 306–315

The Nicotine Metabolite, Cotinine, Alters the Assembly and Trafficking of a Subset of Nicotinic Acetylcholine Receptors

Ashley M. Fox, Faruk H. Moonschi and Christopher I. Richards

J. Biol. Chem. 2015, 290:24403-24412.
doi: 10.1074/jbc.M115.661827 originally published online August 12, 2015